A SCHEMATIC DESIGN AND STRUCTURAL ANALYSIS OF A FUNCTIONALLY GRADED TAPERED SHAFT SYSTEM SUBJECTED TO DIFFERENT STRESSES

BANOTH SUDARSHAN
M.TECH (Machine Design)
Sana Engineering College
Kodad
sudarshan.b@gmail.com

A.KANTHAIAH
Assistant Professor
Sana Engineering College
Kodad
arigelakranthi@gmail.com

ABSTRACT:
Give work bargains the investigation of stresses created in decreased practically evaluated (FG) shaft framework under both warm and mechanical condition for three gestured bar component by utilizing Timoshenko bar hypothesis. The temperature dispersion outspread way is accepted in light of one dimensional relentless state temperature field by Fourier warmth conduction condition without considering heat era. Temperature subordinate material properties are differed along the outspread heading utilizing power law degree. Decreased FG shaft comprises of inflexible plate connected at its middle and shaft is mounted on two adaptable orientation goes about as spring and damper, internal sweep of the decreased shaft is changing in x bearing keeping thickness of empty decreased shaft is consistent. For the present examination the Mixture of Stainless steel (SUS304) and Aluminium oxide (Al2O3) are considered as internal and external surface material of the FG shaft. Three dimensional constitutive relations are determined in view of first request shear misshaping hypothesis (FSDT) for Timoshenko pillar component considering rotating dormancy, strain and active vitality of shaft and gyroscopic impact. In exhibit contemplate basic and hysteretic damping is consolidated. Hamilton's rule is utilized to infer administering condition of movement for three gestured pillar component for six level of flexibility for every hub.

Keywords: *Tapered shaft, functional graded alloys, FE analysis, stress analysis.*

CHAPTER 1
INTRODUCTION

Composite materials will be materials, made out of at least two key materials with various properties, when consolidated to get a material with unexpected properties in comparison to that of individual constituents. Composite material structures are all the more as often as possible utilized as a part of designing fields as their high quality to weight proportion and high solidness to weight proportion is fundamentally positive for material choice. Rule bother with composite material is, deficiency in interface between neighboring layers, which is noticeably known as delamination wonder that may cause essential disillusionment. To crush this issue, another class of material showed, named as Functionally Graded Materials (FGMs). FGMs are seen as, whose material properties are moving toward certain way and in this way vanquish interface weakness.

are portrayed as, the materials whose volume parts of no less than two materials are moved reliably along certain bearing to accomplish required reason. FGMs give better material response and bewildering execution in warm conditions like warm limit and space application, where it is used to shield space convey from warm delivered in the midst of reentry to Earth's air by showing let go material at outside surface metal at inside surface.

virtue of amazing, robustness and low thickness material properties, brings an idea for supplanting customary metallic shafts with FGMs rotor shaft in various application districts like arrangement of turning parts, for instance, driveshaft in automobiles, fly engines and helicopters, turbine shafts and other rotating mechanical assemblies. Composite materials has been endorsed both numerically and likely in rotor stream applications.

Close by this diverse new impelled composite materials and material models for rotor shaft has been delivered by researchers.

CHAPTER 2
LITERATURE REVIEW

2.1 Functionally Graded Materials

Schmauder et al. [2] examined mechanical conduct of ZrO2/NiCr 80 20 sytheses FGMs are broke down and contrasted and exploratory outcomes. And furthermore found that new parameter matricity controls the anxiety level of composite, comprehensively and furthermore locally. Sladek et al. [3] examined time subordinate warmth conduction in nonhomogeneous FGMs. Laplace changes strategy is utilized to take care of beginning limit esteem issue. Results got for limited strip and empty chamber having exponential variety of material properties. Shao et al. [4] exhibited push examination of FG empty round chamber in consolidated mechanical and warm condition by considering straightly expanding temperature. Temperature subordinate material properties are considered and answer for customary differential conditions are unraveled by Laplace changes procedure. Farhatnia et al. [5] introduced push dispersion for composite shaft having FGM in center layer. Temperature subordinate material properties are considered for uniform temperature angle. Jyothula et al. [6] showed nonlinear examination of FGMs in warm condition by changing material assortment parameter, point extent, and cutoff condition re separated with higher demand removing model. Nonlinear synchronous condition are procured by Navier's procedure and conditions are lit up by Newton Raphson iterative method. Callioglu [7] displayed thermoelasticity answer for FG circle. By utilizing microscopic disfigurement hypothesis and power law circulation used to get arrangement. Stress and dislodging variety are displayed along spiral position because of divergent activity, consistent state temperature, inner and outer weight. Abotula et al. [8] examined push field for bending breaks in FGMs for thermo-mechanical stacking. Utilizing strain vitality thickness model impact of ebb and flow parameters, temperature slopes on split development bearings, non-homogeneity esteems are found and examined. Bhandari et al. [9] considered parametric investigation of FGM plate by changing volume portion dispersion and limit conditions. Static investigation of FGM plate has contemplated by sigmoid law and contrasted and writing. Kursun et al. [10] introduced push circulation in a long empty FG chamber under thermomechanical condition. By utilizing minuscule disfigurement hypothesis, answer for dislodging model are found.

2.3 Stresses in FGMs

Charm et al. [11] uncovers impact of thermomechanical coupling in FGMs assumes a critical part. Utilizing von Karman hypothesis, central condition for shallow shells are acquired. Material properties and thermomechanical stretch field are resolved. Reddy and Cheng [12] examined thermomechanical twisting of FG essentially bolstered plates, properties of material are esteemed by Mori-Tanaka plot. Temperature, removal and stress dispersion are figured for various volume part. Jin and Paulino [13] contemplated edge break in a FGM strip under warm condition. Warm properties of FGM fluctuate over thickness bearing, Young's modulus and Poisson's proportion are thought to be steady. Temperature arrangements are acquired for brief time by utilizing Laplace change and asymptotic investigation. Chakraborty et al. [14] inspected push variety in FGMs by utilization of both power law and exponential variety of material properties. New pillar component is produced for behavioral investigation of FGMs. Senthil et al [15] exhibited thermomechanical disfigurement of an essentially upheld FG plate subjected to warm loads on its best and base surfaces. Transient relocation and warm anxieties are gotten for a few basic area of plate subjected to time subordinate temperature and warmth transition. Wang et al. [16] created meshless calculation to mimic warm anxiety circulation in two-dimensional FGMs. Removal segments are controlled by representing conditions and limit condition. Tahani et al. [17] introduced dynamic

qualities of FG thick empty chamber under stacking. Temperature subordinate material properties are viewed as and shift long spiral heading. Dynamic conduct of thermo versatile burdens are examined for different evaluating file. Gupta et al. [18] contemplated dynamic break development conduct of FGMs under transient thermo-mechanical stacking. Principal stress and circumferential stress are discussed and are associated with propagating crack tip.

2.4 Rotor Dynamics

Zorzi and Nelson [19] examined damped rotor solidness including hysteric and inward gooey damping utilizing straight limited component idea. Rouch and Kao [21] exhibited cubic capacity for mass, solidness and gyroscopic grids for a pillar component utilized for transverse relocation. Kim and Bert [22] displayed basic speed of empty tube shaped shaft for overlaid composite materials utilizing slight and thick shell speculations. Gotten comes about are contrasted and traditional shaft hypothesis, comes about are well precise. Bert and Kim [23] presents clasping torque for round and hollow empty covered composite shaft material. Gotten comes about are contrasted and tests, comes about are well precise. Dimarogonas [24] looked into vibration reaction for broke basic part. In view of vibration abundancy and speed of pivot, air out will and close. Singh and Gupta

[25] presented dynamic investigation of composite rotor applying layerwise shaft hypothesis and traditional comparable modulus bar hypothesis. Wettergren and Olsson [26] examined dangers of flat rotor bolstered on adaptable course. Discovered that basic speed can be decreased essentially by interior damping. Abduljabbar et al. [27] introduced dynamic vibration control of adaptable rotor mounted on diary bearing by utilizing criticism controller gadget and sustain forward controller gadget. Reddy and Chin [28] contemplated thermoelastic reaction of FG chambers and plates in powerful in condition. To begin with arrange shear misshapening plate hypothesis is utilized for transverse shear strains, combined with warm conduction condition. Liew et al. [29] dissected thermomechanical conduct of FG chambers. Arrangements are accomplished by novel restricting procedure. Lin et al. [30] presents affectability investigation, dynamic conduct of fast shaft in thermo-mechanical condition. Shaft solidness is resolved for various speed impact, fitting cooling impact and bearing preload. Chang et al. [31] contemplated overlaid composite turning shaft utilizing first request shear distortion hypothesis. Overseeing condition for rotor determined by utilizing Hamilton's

standard. Shokrieh et al. [32] dissected torsional steadiness for pivoting composite shaft. Impact of stacking succession and limit conditions on quality and clasping torque of composite drive shaft has been ascertained utilizing limited component examination. Shao [33] introduced answer for removal, temperature, warm and mechanical worries for FG round empty chamber utilizing multi-layered strategy in view of covered composites show. Temperature subordinate material properties are expected along outspread course and equivalent in each layer. Shao and Ma [34] considered anxiety investigation in FG empty barrel subjected to coupled warm and mechanical condition for straightly shifting temperature field. Applying Laplace change procedure, answer for time subordinate temperature field and thermo mechanical anxiety variety has been figured. Das et al.

[35] studied vibration control of transverse vibration of rotor shaft framework because of unbalance. Vibration control is finished by electromagnets. Xiang and Yang [36] thought about free and compelled vibration of overlaid FG light discharge thickness for thermally induced tensions using TBT. Roy et al. pondered dynamic direct of viscoelastic rotor shaft structure showing inside damping of material. Essential speed of

rotor can be extended by displaying composite material, aluminum framework with carbon fiber. Bayat et al.
[36] [38] displayed thermo adaptable examination for FG turning plates. Temperature subordinate material properties are considered along winding holding on for variable thickness of plate. Badie et al. [39] breaks down typical repeat, catching quality, frustration modes, torsional strength and exhaustion life of composite drive shaft by changing fiber stacking point and presentation edge using constrained segment examination (FEA).
[37] Poursaeidi and Yazdi [40] showed explanations behind silly bends in rotor shaft and amending methods by picking hot spotting process. Sheihlou et al. [41] considered torsional vibration of FG scaled down scale shaft using Hamilton's standard. Vibrations conditions are handled by Galerkin's weighted waiting strategy. Moreover thought about effect of volume bit and farthest point condition on normal repeat and repeat response of scaled down scale FG shaft. Rao et al.
[38] [42] dismembered dynamic lead of FG shaft using TBT. Material properties are believed to be vary according to exponential law. 2.5 Motivation Though composing review reveals an impressive measure of research work has been done on thermo mechanical uneasiness examination of composites and FGMs. Research on extend examination of FG diminished shaft structure in perspective of TBT has not been yet discussed.

MATERIAL MODELLING FOR TAPERED FG SHAF

Material displaying of FG decreased shaft is clarified in detail in this part by taking force law degree and exponential degree.

3.2 Material Modelling of FGMs

Considering FG light emission length and thickness, made of Aluminum Oxide (Al2O3) as an artistic material and Stainless Steel (SUS304) as a metal. Here material are changing along y heading, treating top (y= + h/2) surface as fired and base (y= - h/2) surface as metal. Considering P as a genuine material properties,

P = P V + PV m c

Where Pm , Vm and Pc , Vc are material properties, volume division of metal and earthenware individually. Additionally entirety of volume division of metal (Vm) and volume part of artistic (Vc) are continuously solidarity at any reviewed bearing. It is connected as, **Vm + Vc =1**

3.2.1 Laws of Gradation

There are numerous laws for fluctuating volume part of materials to be specific, control law degree, exponential law of degree, step savvy degree and nonstop degree and so on. Essentially specialists are utilizing power law degree and exponential law.

3.2.1.1 Power Law Gradation

Here volume portion of materials alters along certain course, by utilizing list called as power law file k. This factor controls volume part of any materials and controls shape, quality of material. Figure 3. 1 indicates volume part of metal in FGMS. This is communicated for rectangular piece as,Where $k \geq 0$

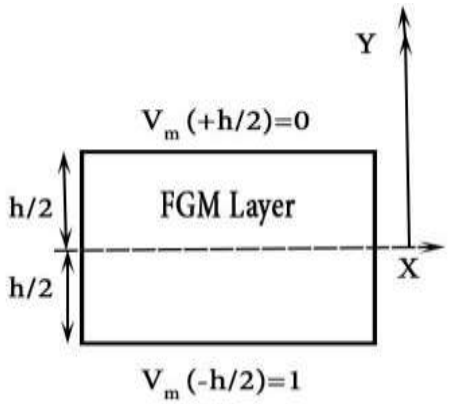

Figure 3. 1 Volume fraction of metal in FGM rectangular cross-section. If p is temperature dependent material properties, it can be written as,

$$P = P_0\left(P_{-1}\theta^{-1} + 1 + P_1\theta + P_2\theta^2 + P_3\theta^3\right)$$

Where P_{-1}, P_1, P_2 and P_3 are temperature coefficients θ^{-1}, θ^1, θ^2 and θ^3 respectively and P_0 material properties at ambient

temperature. Here material properties are function of temperature and certain direction and it is given by,

$$E(y,\theta)=\{E_c(\theta)-E_m(\theta)\}\left(\frac{2y+h}{2h}\right)^k+E_m(\theta)$$

$$\nu(y,\theta)=\{\nu_c(\theta)-\nu_m(\theta)\}\left(\frac{2y+h}{2h}\right)^k+\nu_m(\theta)$$

$$\alpha(y,\theta)=\{\alpha_c(\theta)-\alpha_m(\theta)\}\left(\frac{2y+h}{2h}\right)^k+\alpha_m(\theta)$$

$$\rho(y)=(\rho_c-\rho_m)\left(\frac{2y+h}{2h}\right)^k+\rho_m$$

Density is assumed to be not dependent on temperature and it is vary along certain directions only.

3.2.1.2 Exponential Law of Gradation

In this gradation material properties are vary along certain directions as,

$$P(y)=P_0e^{k\left(y+\frac{h}{2}\right)}$$

Where P0 indicates, base surface material properties of FGM, "k" is the factor which controls degree crosswise over thickness 'h'. Youthful's modulus warm conductivity, coefficient of warm extension and thickness of the FG material are given as,
This straightforward govern of blend is expect toxic substance's proportion is steady.

3.3 Modelling of Material Properties Applicable To tapered FG Shaft

Decreased shaft with limited length L, inward span at starting and end of shaft are R0 and R1 individually having consistent thickness of t all through the decreased shaft. Top surface of shaft is of fired rich and internal surface of shaft is metal rich

$$E(y)=E_0e^{k\left(y+\frac{h}{2}\right)} \qquad \alpha(y)=\alpha_0e^{k\left(y+\frac{h}{2}\right)}$$

$$K(y)=K_0e^{k\left(y+\frac{h}{2}\right)} \qquad \rho(y)=\rho_0e^{k\left(y+\frac{h}{2}\right)}$$

Figure 3. 2 Volume fraction of metal in tapered FG shaft

CHAPTER 4

FORMULATION FOR TAPERED FG SHAFT

4.1 Introduction

FG decreased shaft comprises of three gestured Timoshenko bar, in view of the First request shear distortion hypothesis considering both Gyroscopic and rotating dormancy impact. Empty roundabout cross segment shaft is considered for examination and it is pivoting about its longitudinal hub. Figure 4. 1 demonstrates dislodging factors and Figure 4. 2 indicates graph speaking to the pole.

4.2 Finite Element Modelling of Shaft

FG turning shaft has demonstrated utilizing Finite component technique for three gestured Timoshenko pillar component having six degrees of opportunity at every hub. By applying direct flexible and little redirection hypothesis is accepted in exhibit work.
Accepted dislodging field as given beneath [31]

$$\left.\begin{aligned}u_x(x,y,z,t)&=u(x,t)+z\beta_x(x,t)-y\beta_y(x,t)\\u_y(x,y,z,t)&=v(x,t)-z\phi(x,t)\\u_z(x,y,z,t)&=w(x,t)+y\phi(x,t)\end{aligned}\right\}$$

Strain-displacement relations can be written in Cartesian coordinate system as,

$$\left.\begin{aligned}\varepsilon_{xx}&=\frac{\partial u}{\partial x}+z\frac{\partial\beta_x}{\partial x}-y\frac{\partial\beta_y}{\partial x};\quad \varepsilon_{xy}=\frac{1}{2}\left(-\beta_y+\frac{\partial v}{\partial x}-z\frac{\partial\phi}{\partial x}\right)\\\varepsilon_{xz}&=\frac{1}{2}\left(\beta_x+\frac{\partial w}{\partial x}+y\frac{\partial\phi}{\partial x}\right);\quad \varepsilon_{yy}=\varepsilon_{zz}=\varepsilon_{yz}=0\end{aligned}\right\}$$

These strain relations can be changed in to round and hollow organize framework by utilizing change grid. Strain-relocation relations would now be able to be composed in tube shaped facilitate framework by taking y = r cosθ, z = r sinθ, m = cosθ and n = sinθ.

$$\varepsilon_{xx}=\frac{\partial u}{\partial x}+r\sin\theta\frac{\partial\beta_x}{\partial x}-r\cos\theta\frac{\partial\beta_y}{\partial x};\quad \varepsilon_{rr}=\varepsilon_{\theta\theta}=\varepsilon_{r\theta}=0$$

$$\varepsilon_{x\theta}=\frac{1}{2}\left(\beta_y\sin\theta+\beta_x\cos\theta-\sin\theta\frac{\partial v}{\partial x}+\cos\theta\frac{\partial w}{\partial x}+r\frac{\partial\phi}{\partial x}\right)$$

$$\varepsilon_{xr}=\frac{1}{2}\left(\beta_x\sin\theta-\beta_y\cos\theta+\sin\theta\frac{\partial w}{\partial x}+\cos\theta\frac{\partial v}{\partial x}\right)$$

And the above strain displacement relations in cylindrical coordinate can be written in matrix form as,

$$\begin{Bmatrix}\varepsilon_{xx}\\ \gamma_{x\theta}\\ \gamma_{xr}\end{Bmatrix}=\frac{1}{2}\begin{bmatrix}2\frac{\partial}{\partial x} & 0 & 0 & 2r\sin\theta\frac{\partial}{\partial x} & -2r\cos\theta\frac{\partial}{\partial x} & 0\\ 0 & -\sin\theta\frac{\partial}{\partial x} & \cos\theta\frac{\partial}{\partial x} & \cos\theta & \sin\theta & r\frac{\partial}{\partial x}\\ 0 & \cos\theta\frac{\partial}{\partial x} & \sin\theta\frac{\partial}{\partial x} & \sin\theta & -\cos\theta & 0\end{bmatrix}\begin{Bmatrix}u\\ v\\ w\\ \beta_x\\ \beta_y\\ \phi\end{Bmatrix}$$

Stress strain relations in any layer of the FG shaft can be written as [31]

$$\begin{Bmatrix}\sigma_{xx}\\ \tau_{x\theta}\\ \tau_{xr}\end{Bmatrix}=\begin{bmatrix}C_{11r} & k_sC_{16r} & 0\\ k_sC_{16r} & k_sC_{66r} & 0\\ 0 & 0 & k_sC_{55r}\end{bmatrix}\begin{Bmatrix}\varepsilon_{xx}\\ \gamma_{x\theta}\\ \gamma_{xr}\end{Bmatrix}$$

Where k_s is the shear correction factor and C_{ijr} represents constitutive element, related to elastic constants for transversely isotropic material.Coupled (thermo-mechanical) stress strain relations in any layer of FG shaft can be written as,

$$\begin{Bmatrix}\sigma_{xx}\\ \tau_{x\theta}\\ \tau_{xr}\end{Bmatrix}=\begin{bmatrix}C_{11r} & k_sC_{16r} & 0\\ k_sC_{16r} & k_sC_{66r} & 0\\ 0 & 0 & k_sC_{55r}\end{bmatrix}\left\{\begin{Bmatrix}\varepsilon_{xx}\\ \gamma_{x\theta}\\ \gamma_{xr}\end{Bmatrix}-\begin{bmatrix}\alpha\Delta T\\ 0\\ 0\end{bmatrix}\right\}$$

4.2.1 Kinetic Energy Expression of Shaft

The effect of both rotary and translation of FG shaft are considered for deriving kinetic energy expression, it is written as,

$$T_s=\frac{1}{2}\int_0^L\left[\begin{matrix}I_m(\dot u^2+\dot v^2+\dot w^2)+I_d(\dot\beta_x^{\,2}+\dot\beta_y^{\,2})-2\Omega I_p\beta_x\dot\beta_y\\ +I_p\dot\phi^2+2\Omega I_p\dot\phi+\Omega^2I_p+\Omega^2I_d(\beta_x^{\,2}+\beta_y^{\,2})\end{matrix}\right]dx$$

pole, L is length of the pole, Ip, Im and Id are polar mass snapshot of idleness, mass snapshot of latency and polar mass snapshot of dormancy separately. In above condition ignoring some little terms, first variety of active vitality is composed as,

$$\delta T_s=\int_0^L\left[\begin{matrix}I_m\left(\dot u\frac{\partial\delta u}{\delta t}+\dot v\frac{\partial\delta v}{\delta t}+\dot w\frac{\partial\delta w}{\delta t}\right)+I_d\left(\dot\beta_x\frac{\partial\delta\beta_x}{\delta t}+\dot\beta_y\frac{\partial\delta\beta_y}{\delta t}\right)\\ +I_p\dot\phi\delta\dot\phi+\Omega I_p\delta\dot\phi-\Omega I_d\left(\beta_x\frac{\partial\delta\beta_y}{\delta t}+\dot\beta_y\delta\beta_x\right)\end{matrix}\right]dx$$

4.2.2 Strain Energy Equation for FG Shaft

Strain energy of FG shaft is given by,

$$U_s=\frac{1}{2}\int_V\{\sigma\}^T\{\varepsilon\}dV=\frac{1}{2}\int_V(\sigma_{xx}\varepsilon_{xx}+\sigma_{rr}\varepsilon_{rr}+\sigma_{\theta\theta}\varepsilon_{\theta\theta}+2\tau_{xr}\varepsilon_{xr}+2\tau_{x\theta}\varepsilon_{x\theta}+2\tau_{r\theta}\varepsilon_{r\theta})dV$$

As $\varepsilon_{rr}=\varepsilon_{\theta\theta}=\varepsilon_{r\theta}=0$

Strain energy can be rewritten as,

$$U_s=\frac{1}{2}\int_V(\sigma_{xx}\varepsilon_{xx}+2\tau_{xr}\varepsilon_{xr}+2\tau_{x\theta}\varepsilon_{x\theta})dV$$

.2.3 Kinetic energy expression for disks on shaft

Disks fixed on shaft are treated as isotropic material. Expression for kinetic energy of disks is written as,

$$T_d=\frac{1}{2}\int_0^L\sum_{i=1}^{N_D}\left[\begin{matrix}I_{mi}^D\left(\dot u^2+\dot v^2+\dot w^2\right)+I_{di}^D\left(\dot\beta_x^{\,2}+\dot\beta_y^{\,2}\right)\\ -2\Omega I_{di}^D\beta_x\dot\beta_y+I_{pi}^D\dot\phi^2+2\Omega I_{pi}^D\dot\phi+\Omega^2I_{pi}^D\end{matrix}\right]\Delta(x-x_{Di})dx$$

Where $I_{mi}^{\,D}$, $I_{di}^{\,D}$ and $I_{\,pi}^{\,D}$ mass moment of inertia, diametrical and polar mass moment of inertia of i^{th} disk respectively. The term $\Delta\left(x-x_{Di}\right)$ represents one dimensional spatial Dirac delta function. x_{Di} gives location i^{th} disk and N_D is the number of disks which are attached to shaft. Variation of the kinetic energy of disk given by,

$$\delta T_d=\int_0^L\sum_{i=1}^{N_D}\left[\begin{matrix}I_{mi}^D\left(\dot u\frac{\partial\delta u}{\delta t}+\dot v\frac{\partial\delta v}{\delta t}+\dot w\frac{\partial\delta w}{\delta t}\right)+I_{di}^D\left(\dot\beta_x\frac{\partial\delta\beta_x}{\delta t}+\dot\beta_y\frac{\partial\delta\beta_y}{\delta t}\right)-\\ \Omega I_{pi}^D\left(\dot\beta_y\delta\beta_x+\beta_x\frac{\partial\delta\beta_y}{\delta t}\right)+I_{pi}^D\dot\phi\delta\dot\phi+I_{pi}^D\Omega\delta\dot\phi\end{matrix}\right]\Delta(x-x_{Di})dx \quad (28)$$

4.3 Contribution of internal damping-By including both internal viscous and hysteresis damping [19] of shaft and disk elements extended final

equation of motion can written as, Where K_{cir} is the skew-symmetric circulation matrix .

5.2 Validation of Code

To confirm the created code, uniform shaft made of graphite epoxy composite material with plate at focus of shaft [31] (measurements are in Table 5. 5). Gotten comes about are well concurrence with writing. Figure 5. 1 demonstrates Campbell outline for initial four sets of modes achieved a superb match with distributed outcome [31].

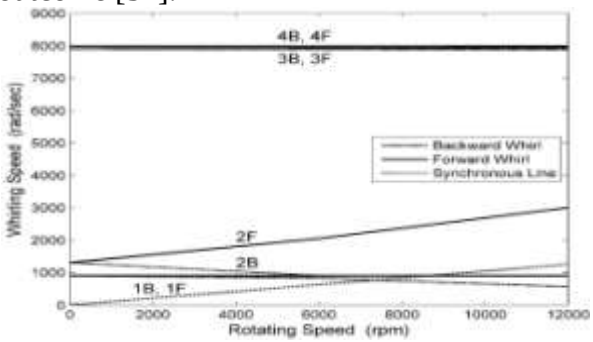

Figure 5.1 Campbell diagram for laminated graphite-epoxy composite material.

5.3 Temperature Distribution in Tapered FG Shaft

Temperature variety in decreased FG shaft is appeared in Figure 5. 2. As material properties are elements of temperature and spiral bearing, displayed here temperature appropriation. This variety is because of warm conductivity, CTE, youthful's modulus of material. Temperature variety is acquired at waist of decreased shaft, it is watched that, for k zero to one temperature diminishes bit by bit and k more noteworthy than one temperature increments.

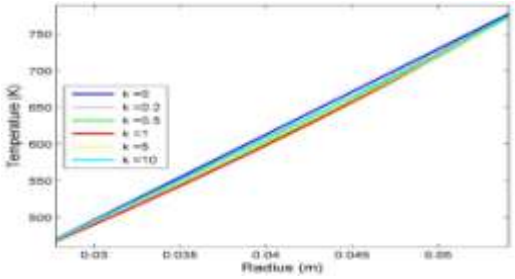

Figure 5.2 Temperature variety in waist of decreased FG shaft.

5.4 Material properties of tapered FG shaft depends on temperature and power law index

Decreased FG shaft is displayed by taking Aluminum oxide as an earthenware and Stainless steel as a metal, these are rich at best and base surfaces separately. Figure 5. 3 demonstrates volume part of clay material of FGM. Properties of material are changes along span of shaft, here power law file is noteworthy factor. As per above thought and plan, as "k" esteem ways to deal with zero, material turns out to be completely artistic and as "k" esteem ways to deal with vastness material turns out to be completely metal. Straight variety of material is gotten by taking k=1. Since shaft is in warm condition, it is important to discover properties rely upon temperature. Figure 5.4 Figure 5.5 and Figure 5.6 are modulus versatility, Poisson's proportion and coefficient of warm extension individually. Here properties are changing for every component as investigation is advanced.

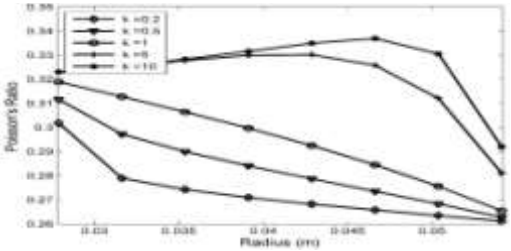

Figure 5. 5 Variation of Poisson's ratio along radius for power law index.

5.5 Stress analysis in tapered FG shaft

Target of present examination is to investigate the coupled thermo-mechanical worries in decreased FG shaft. At first relative investigation of FG shaft has completed over steel shaft. At that point, push comes about are plotted for various estimations of energy law record and speed and furthermore time subordinate anxiety are likewise introduced.

5.5.1 Comparative investigation of decreased FG shaft over steel decreased shaft

It is basic to look at consequences of stainless steel and FG shaft to indicate impacts of FG shaft over steel shaft. In this near investigation area temperature

accepted is direct. Material properties are elements of temperature and outspread bearing as it were. Keeping all parameters (as in Table 5. 1) are same for both FG and steel investigation is finished. Figure 5.7 shows run of the mill and shear stress in x and theta bearing independently for Stainless steel material. Conventional tension is extending along traverse conflictingly; shear extend also growing along clear unequivocally. Figure 5.8 and Figure 5.9 shows run of the mill and shear stress in x and theta course exclusively for FGM.

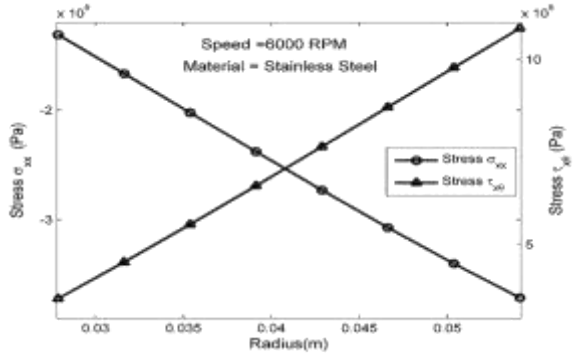

Figure 5.7 Stress created in decreased Steel shaft along range are shown for

shaft running at 6000 RPM, particular "k" values. It is easily seen from Figures that, extend made in FG shaft is lesser than Stainless steel shaft close outer surface of shaft this conclusion effect to consider FGMs.

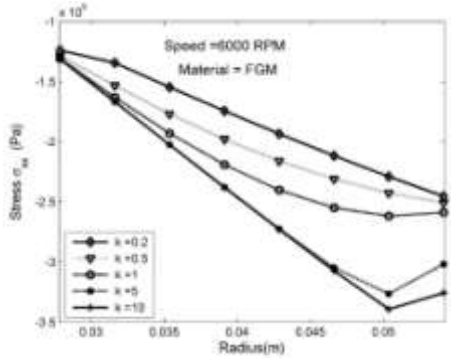

Figure 5. 8 Normal stress in tapered FG shaft along radius.

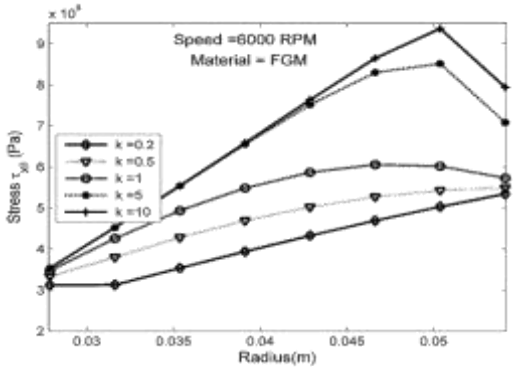

Figure 5. 9 Shear stress in tapered FG shaft along radius.

5.5.2 Variation of stresses for different values of 'k' in radial direction

In coupled warm and mechanical condition, warm strain is in combined with just typical anxiety and shear worry in theta course as in condition (21). Temperature subordinate material properties are considered and temperature variety is as appeared in Figure 5. 2. Figure 5. 10 (an) and (b) demonstrates typical weight on plane opposite to x hub in x heading at 6000 RPM and 12000 RPM individually. Most extreme anxiety esteem is acquired at time t=0.008 sec and t=0.044 sec for 6000 RPM and 12000 Rpm separately. Stress increments along range of shaft contrarily as warm anxiety commands mechanical worry in coupled condition. Likewise considering at a specific span, ordinary anxiety is increments as "k" esteem increments, since volume portion of steel material is increments as power law file (k) increments. Fig (an) and Fig (b) are practically same yet distinction is, as speed expands abundancy in push is more, which is appeared and clarified in succeeding segment.

Figure 5. 10 (an) and (b) indicates shear weight on plane opposite to x pivot in theta bearing at 6000 RPM and 12000 RPM individually. Most extreme anxiety esteems are acquired at time t=0.008 sec and t=0.044 sec for 6000 RPM and 12000 Rpm separately. Shear stretch increments along sweep of shaft decidedly as warm anxiety commands mechanical worry in coupled condition. Likewise considering a specific span, shear stretch is increments as "k" esteem increments, since volume part of

steel material is increments as power law file (k) increments. Fig (an) and Fig (b) are practically same however contrast is, as speed builds change in push is more, which is appeared and clarified in succeeding segment.

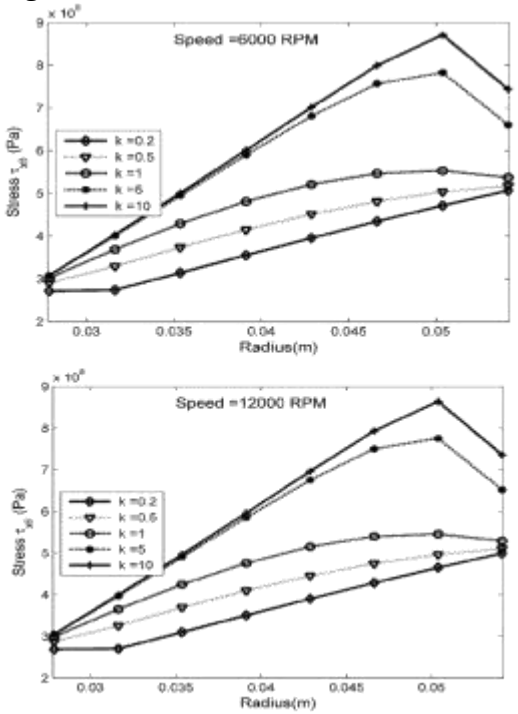

Figure 5. 11 Shear stress in tapered FG shaft along radius.(a) At 6000 RPM, (b) at 12000 RPM

5.5.3 Transient uncoupled stress analysis for different value of power law index

Uncoupled (without considering warm strain) transient anxiety acquired by condition (20) at the highest point of the surface. Considering temperature subordinate material properties and temperature variety as in Figure 5. 2. Figure 5. 12 Shows ordinary weight on plane opposite to x hub in x course, Figure 5. 13 and Figure 5. 14 demonstrates shear weight on plane opposite to x pivot in theta and outspread course individually likewise (an) and (b) speaks to shaft running at 6000 RPM and 12000 RPM separately. Greatest anxiety adequacy created in decreased shaft for beginning little time interim, at that point push abundancy is diminishes as time increments and keep up consistent plentifulness at speed 6000 RPM. For starting little time interim anxiety abundancy is littler, as time expands stretch sufficiency builds at that point achieves practically steady adequacy for shaft running at 12000 RPM. Additionally it can be seen that, as power law list builds push abundancy expands, this depends on relocation. Likewise by taking a gander at y hub esteems, stretch abundancy increments as speed increments.

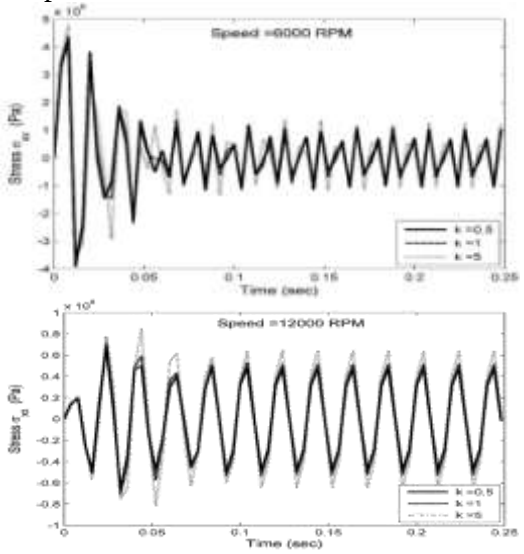

Figure 5. 12 Transient uncoupled normal stress in tapered FG shaft:
(a) At 6000 RPM, (b) at 12000 RPM

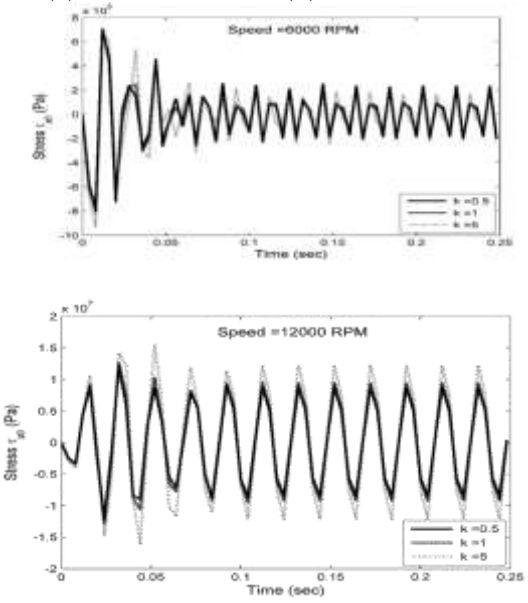

Figure 5. 13 Transient uncoupled shear stress in tapered FG shaft in theta direction:
(a) At 6000 RPM, (b) at 12000 RPM

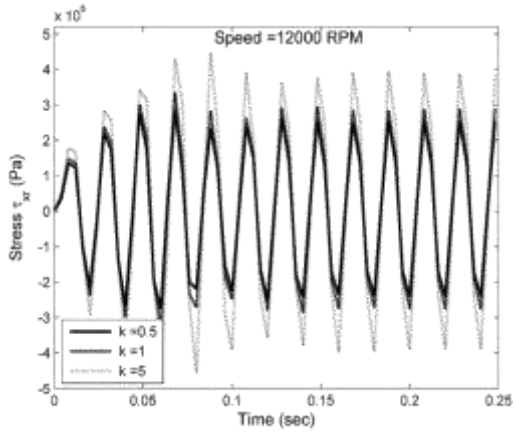

Figure 5. 14 Transient uncoupled shear stress in tapered FG shaft in radial direction:(a) At 6000 RPM, (b) at 12000 RPM

5.5.4 Transient coupled stress analysis for different value of power law index

Coupled (with considering warm strain) transient anxiety acquired by condition (21) at the highest point of the surface. Considering temperature subordinate material properties and temperature variety as in Figure 5. 2. Figure 5. 15 Shows ordinary weight on plane opposite to x hub in x heading, Figure 5. 16 demonstrates shear weight on plane opposite to x pivot in theta heading moreover

(a) and (b) speaks to shaft running at 6000 RPM and 12000 RPM separately. Most extreme anxiety sufficiency created in decreased shaft for beginning little time interim, at that point push plentifulness is diminishes as time increments and keep up consistent adequacy at speed 6000 RPM. For beginning little time interim anxiety plentifulness is littler, as time expands stretch sufficiency builds at that point accomplishes practically consistent adequacy for shaft running at 12000 RPM. Likewise it can be seen that, as power law record expands stretch abundancy builds, this depends on dislodging. Additionally by taking a gander at y hub esteems, push sufficiency increments as speed increments.

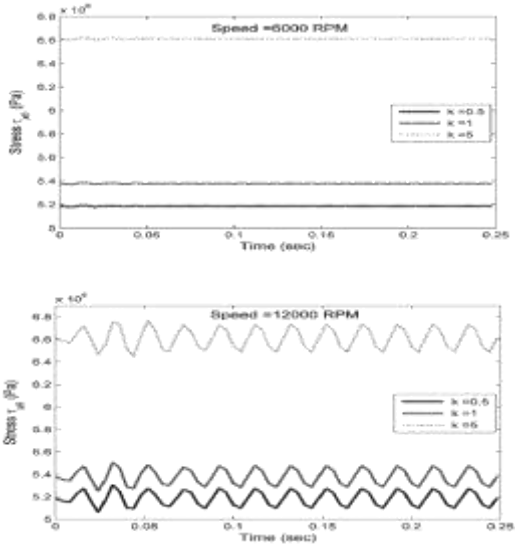

Figure 5. 16 Transient coupled shear stress in tapered FG shaft in theta direction: (a) At 6000 RPM, (b) At 12000 RPM

ANSYS RESULTS

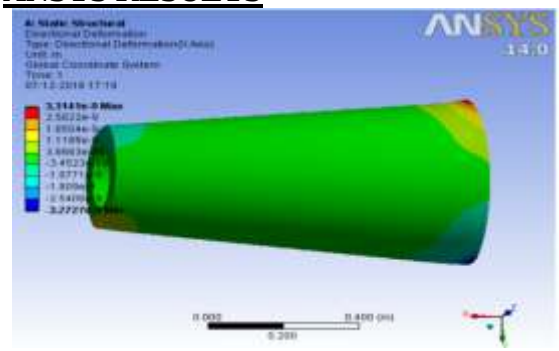

DIRECTIONAL DEFORMATION

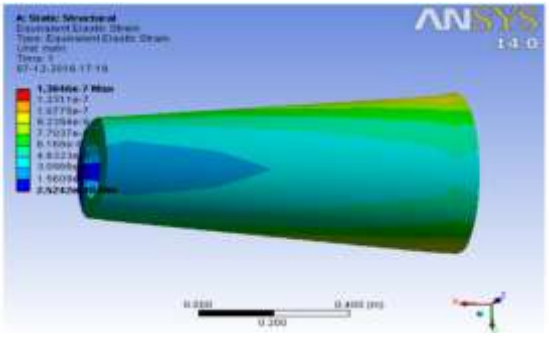

ELASTIC STRAIN

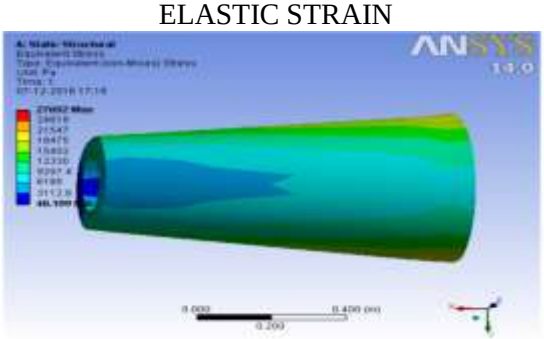

EQUIVALENT STRESS

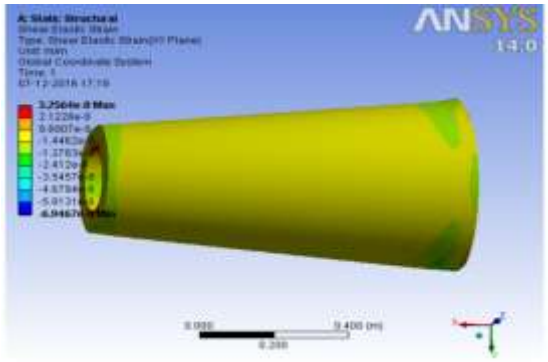

SHEAR ELASTIC STRAIN

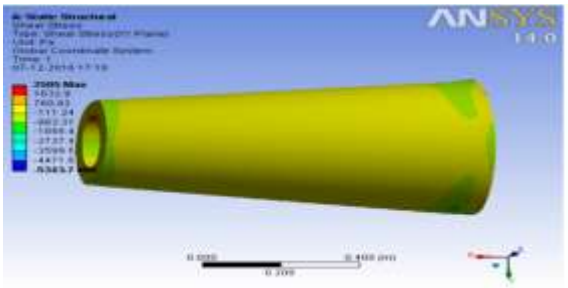

SHEAR STRESS

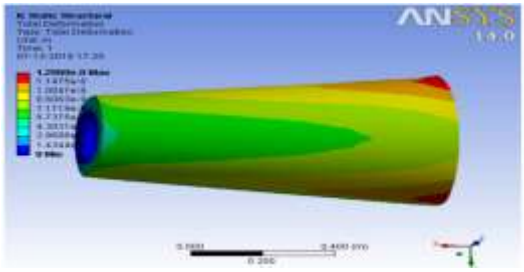

TOTAL DEFORMATION

CHAPTER 6
CONCLUSION AND SCOPE OF FUTURE WORK

Imperative conclusions are attracted this part in light of above talked about outcomes. Chance of future work is likewise been exhibited in this part.

6.1 Conclusions

Display think about backings to make following vital determinations.

i. Three gestured Timoshenko pillar component has been executed for displaying and investigation of FG decreased shaft by assessing auxiliary damping and hysteretic damping in temperature condition.

ii. The temperature dissemination is expected in light of one Dimensional unfaltering state temperature field by utilizing Fourier warmth conduction condition without considering heat era.

iii. Temperature subordinate material properties are set up by taking diverse power law list esteem.

iv. Stress esteems are looked at amongst steel and FG shaft by taking temperature subordinate material properties for direct variety of temperature, it is discovered that anxieties created in FG shaft is lower than Steel shaft. Additionally for better outcomes we utilize the ANSYS programming for contrasting outcomes.

References

1. *Sankar, B. V., and Tzeng, J. T., 2002, "Warm Stresses in Functionally Graded Beams," AIAA J., 40, pp. 1228– 1232.*

2. *Sankar, B. V., 2001, "An Elasticity Solution for Functionally Graded Beams," Compos. Sci. Technol., 61, pp. 689– 696.*

3. *Apetre, N. A., Sankar, B. V., and Ambur, D. R., 2006, "Low-Velocity Impact of Sandwich Beams With Functionally Graded Core," Int. J. Solids Struct., 43, pp. 2479– 2496.*

4. *Bhangale, R. K., and Ganesan, N., 2006, "Thermoelastic Buckling and Vibration Behavior of a Functionally Graded Sandwich Beam With Constrained Viscoelastic Core," J. Sound Vib., 295, pp. 294– 316.*

5. *Conde, Y., Pollien, An., and Mortensen, A., 2006, "Utilitarian Grading of Metal Foam Cores for Yield-Limited Lightweight Sandwich Beams," Scr. Mater., 54, pp. 539– 543.*

6. *Chakraborty, A., Gopalakrishnan, S., and Reddy, J. N., 2003, "A New Beam Finite Element for the Analysis of Functionally Graded Materials," Int. J. Mech. Sci., 45, pp. 519– 539.*

7. *Chakraborty, An., and Gopalakrishnan, S., 2003, "A Spectrally Formulated Finite Element for Wave Propagation Analysis in Functionally Graded Beam," Int. J. Solids Struct., 40, pp. 2421– 2448.*

8. *Ching, H. K., and Yen, S. C., 2006, "Transient Thermoelastic Deformation of 2-D Functionally Graded Beams Under Nonuniformly Convective Heat Supply," Compos. Struct., 73, pp. 381– 393.*

9. *Tsukamoto, H., 2003, "Expository Method of Inelastic Thermal Stresses in a Functionally Graded Material Plate by a Combination of Micro- and Macromechanical Approaches," Composites, Part B, 34, pp. 561– 568.*

10. Ootao, Y., and Tanigawa, Y., 1999, "Three-Dimensional Transient Thermal Stresses of Functionally Graded Rectangular Plate Due to Partial Heating," J. Therm. Stresses, 22, pp. 35– 55.

11. Zimmerman, R. W., and Lutz, M. P., 1999, "Warm Stresses and Thermal Expansion in a Uniformly Heated Functionally Graded Cylinder," J. Therm. Stresses, 22, pp. 178– 188.

12. Pitakthapanaphong, S., and Busso, E. P., 2002, "Self-Consistent Elastoplastic Stress Solutions for Functionally Graded Material Systems Subjected to Thermal Gradients," J. Mech. Phys. Solids, 50, pp. 695– 716.

13. Reddy, J. N., 2000, "Examination of Functionally Graded Plates," Int. J. Numer. Strategies Eng., 47, pp. 663– 684.

14. Reddy, J. N., and Cheng, Z.- Q., 2001, "Three-Dimensional Thermomechanical Deformations of Functionally Graded Rectangular Plates," Eur. J. Mech. A/Solids, 20, pp. 841– 855.

15. Reddy, J. N., and Chen, C. D., 1998, "Thermo mechanical Analysis of Functionally Graded Cylinders and Plates," J. Therm. Stresses, 21, pp. 593– 626.

16. Praveen, G. N., and Reddy, J. N., 1998, "Nonlinear Transient Thermoelastic Analysis of Functionally Graded Ceramic-Metal Plates," Int. J. Solids Struct., 35, pp. 4457– 4476.

17. Loy, C. T., Lam, K. Y., and Reddy, J. N., 1999, "Vibration of Functionally Graded Cylindrical Shells," Int. J. Mech. Sci., 41, pp. 309– 324.

18. Praveen, G. N., Chin, C. D., and Reddy, J. N., 1999, "Thermoelastic Analysis of Functionally Graded Ceramic-Metal Cylinder," J. Eng. Mech., 125, pp. 1259– 1267.

19. Pradhan, S. C., Loy, C. T., Lam, K. Y., and Reddy, J. N., 2000, "Vibration Characteristics of Functionally Graded Cylindrical Shells Under Various Boundary Conditions," Appl. Acoust., 61, pp. 119– 129.

20. Reddy, J. N., Wang, C. M., and Kitipornchai, S., 1999, "Axysimmetric Bending of Functionally Graded Circular and Annular Plates," Eur. J. Mech. A/Solids, 18, pp. 185– 199.

21. Vel, S. S., and Batra, R. C., 2004, "Three Dimensional Exact Solution for the Vibration of Functionally Graded Rectangular Plates," J. Sound Vib., 272, pp. 703– 730.

22. Vel, S. S., and Batra, R. C., 2003, "Three-Dimensional Analysis of Transient Thermal Stresses in Functionally Graded Plates," Int. J. Solids Struct., 40, pp. 7181– 7196.

23. Qian, L. F., and Batra, R. C., 2004, "Transient Thermoelastic Deformations of a Thick Functionally Graded Plate," J. Therm. Stresses, 27, pp. 705– 740.

24. Qian, L. F., Batra, R. C., and Chen, L. M., 2004, "Static and Dynamic Deformation of Thick Functionally Graded Elastic Plates by Using Higher-Order Shear and Normal Deformable Plate Theory and Meshless Local Petrov– Galerkin Method," Composites, Part B, 35, pp. 685– 697.

25. Kashtalyan, M., 2004, "Three Dimensional Elasticity Solution for Bending of Functionally Graded Rectangular Plates," Eur. J. Mech. A/Solids, 23, pp. 853– 864.

26. Elishakoff, I., and Gentilini, C., 2005, "Three-Dimensional Flexure of Rectangular Plates Made of Functionally Graded Materials," ASME J. Appl. Mech., 72, pp. 788– 791.

27. Pan, E., 2003, "Correct Solution for Functionally Graded Anisotropic Elastic Composite Laminates," J. Compos. Mater., 37, pp. 1903– 1919.

28. Soldatos, K. P., 2004, "Complex Potential Formalisms for Bending of Inhomogeneous Monoclinic Plates Including Transverse Shear Deformations," J. Mech. Phys. Solids, 52, pp. 341– 357.

29. Croce, L. D., and Venini, P., 2004, "Limited Elements for Functionally Graded Reissner-Mindlin Plates," Comput.